Eur. Phys. J. C 51, 135–148 (2007)
DOI 10.1140/epjc/s10052-007-0281-z

THE EUROPEAN PHYSICAL JOURNAL C

Regular Article – Theoretical Physics

The Gibbs equilibrium conditions applied to the QGP–hadron transition curve

A.S. Kapoyannis[a]

University of Athens, Physics Department, Nuclear and Particle Physics Section, Panepistimioupolis, Ilissia, 15771 Athens, Greece

Received: 18 April 2006 / Revised version: 17 November 2006 /
Published online: 6 April 2007 –

Abstract. A method is developed to consistently satisfy the Gibbs equilibrium conditions between the quark–gluon and hadronic phase, although each phase has been formulated in separate grand canonical partition functions containing three quark flavours. The sector in the space of thermodynamic variables where the transition takes place is restricted to a curve, according to the phase diagram of QCD. The conservation laws of quantum numbers are also imposed on the transition curve. The effect of the inclusion of the pentaquark states is considered. The data from S + S, S + Ag (SPS) and Au + Au (RHIC) are found to be compatible with the formation of a QGP phase and the occurrence of the chemical freeze-out immediately after crossing the transition line, but the data from Pb + Pb (SPS) are not.

PACS. 12.40.Ee; 05.70.Fh; 12.38.Mh; 24.10.Pa

1 Introduction

Quantum chromodynamics is universally accepted as the theory of the strong interactions. Within the context of this theory the quark–gluon plasma phase receives an accurate description. However, the formation of the hadronic phase, which is the final state of any possible primordial QGP state, still remains an open problem in view of QCD. On the other hand, the hadronic multiplicities emerging from heavy-ion collisions have been extensively and successfully predicted by statistical models using a handful of thermodynamical parameters [1–15]. So the use of two separate models for the QGP and the hadron phase, called a hadron gas (HG), offers a complementary approach.

Effective model calculations based on QCD predict that the transition between QGP and the hadronic phase is a first order one at high baryon densities (depicted by a critical line on the (T, μ_B) plane), while it is of higher order at low or zero baryon densities (crossover). The end point of the first order transition line is a critical point [16–18]. The transition points must be restricted to a curve on the phase diagram of temperature and chemical potential of the baryon. In view of this aspect any models to be used for the description of QGP and HG have to be matched properly at the transition between the two phases.

The aim of this work is to trace the sector of the space of thermodynamic variables where the QGP–hadron transition occurs, with the following requirements.

(a) Any mixed phase formed in the first order part of the transition must occupy only a curve in the space of the thermodynamic variables. This requirement is even stronger in the crossover area where a mixed phase does not exist.
(b) The Gibbs equilibrium conditions have to be satisfied, which amount to $T_{\mathrm{QGP}} = T_{\mathrm{HG}}$ for thermal equilibrium, $P_{\mathrm{QGP}} = P_{\mathrm{HG}}$ for mechanical equilibrium and $\{\mu\}_{\mathrm{QGP}} = \{\mu\}_{\mathrm{HG}}$ for chemical equilibrium, where $\{\mu\}$ stands for the set of chemical potentials used in the description of the two phases.
(c) All the conservation laws of quantum numbers like baryon number B, electric charge Q, strangeness S, etc. have to be satisfied at every point on the transition line, in a way that they could be extended for every number of flavours that are present in the system.

One is confronted with these problems every time separate partition functions are used for the two phases, but the simultaneous fulfillment of the above conditions has not been achieved. Among the numerous examples that exist, in [19], where only light, identical quarks are used ($u = d \equiv q$), the curves of equal pressures are made to approximately coincide by the choice of the external parameters B and a_s, something which does not allow for matching when other flavours are introduced. In [20] the strange fugacity λ_s is discontinuous at the HG–QGP transition, and the conservation of baryon number can only be accommodated in the case of a first order transition. In [21] the strange chemical potential μ_s is also discontinuous. In [22] only q quarks are considered, and the requirement of the continuity of the chemical potentials and conservation of baryon number leads to a mixed phase which occupies a surface and

[a] e-mail: akapog@phys.uoa.gr

not a line on the (T, μ_B) plane. The same is true in [23–25] where also s quarks are included. In [26] there is an analogous situation as in [22] with a critical line at the (T, μ_B) plane, but the conservation of baryon number is not considered. In [27] the q and s quark chemical potentials are continuous, but baryon number and strangeness of the system are not kept constant during hadronisation, since hadrons evaporate from the QGP. The considerations of [20–27] are consistent with a first order transition but cannot be valid at the crossover region. In this work all the thermodynamic variables and the pressure will be kept continuous at the transition line (in contrast with [19–21]), and the first order part of the transition will be presented by a line on the (T, μ_B) plane (different from [22–25]), and no evaporation of hadrons will be assumed from the system (different from [27]).

Let us consider the requirements that a system with N_f quark flavours has to satisfy. Every conservation law accounts for two equations to be fulfilled. One sets the value of the quantum quantity, e.g. $\langle B\rangle_{\rm QGP} = b_i$, and the other one assures the conservation at the phase transition, e.g. $\langle B\rangle_{\rm QGP} = \langle B\rangle_{\rm HG}$. The total number of equations that must hold is, thus, $2N_f + 1$ (the unit accounts for the equality of pressures). Assuming the existence of full chemical equilibrium, every quark flavour introduces one extra fugacity in the set of thermodynamical variables, which, with the inclusion of volume and temperature, amount to $N_f + 2$. At the crossover region, the surviving free parameters required to fulfill the necessary equations decrease to $N_f + 1$, because of the equality of densities and consequently the equality of volumes between the two phases ($V_{\rm QGP} = V_{\rm HG}$). At the first order transition line the free parameters are $N_f + 2$, since now $V_{\rm QGP} \neq V_{\rm HG}$. It is evident, then, that the necessary $2N_f + 1$ conditions can be fulfilled only at the first order part of the transition and only when there is one flavour present, $N_f = 1$, or when the u and d quarks are considered identical (q quarks, described by a single chemical potential μ_q). It has to be emphasised that the conditions like $\langle B\rangle_{\rm QGP} = b_i$ have to be satisfied in order to have a whole line of transition points. If these equations are dropped, then we are left with $N_f + 1$ equations, which can be solved but result in a unique point in the space of the thermodynamical parameters.

2 Expanding the fugacity sector

It is clear that in order to satisfy $2N_f + 1$ relations, every flavour has to be accompanied by two fugacities instead of one. The multiplicity data emerging from heavy-ion collisions suggest that the thermalised hadronic system has not achieved full chemical equilibrium. First the partial chemical equilibrium factor of the strangeness γ_s had been introduced [2, 3] and used extensively to model the data [4–8]. Also a similar factor for the light quarks γ_q was introduced [9] and used in certain analyses [10, 11]. Here the light u and d quarks will be accompanied by separate fugacities γ_u, γ_d. A factor γ_j controls the quark density $n_j + n_{\bar{j}}$ [4] in contrast with the usual fugacity λ_j, which controls the net quark density $n_j - n_{\bar{j}}$. These additional fugacities can serve the purpose of satisfying the necessary equations at the transition point, as well as preserving the continuity of the chemical potentials between the two phases.

A system with three flavours (u, d and s quarks) is described by the set of thermodynamical variables $(T, \lambda_u, \gamma_u, \lambda_d, \gamma_d, \lambda_s, \gamma_s) \equiv (T, \{\lambda, \gamma\})$. Setting $x = V_{\rm HG}/V_{\rm QGP}$, the set of equations to be satisfied at every phase transition point will be

$$P_{\rm QGP}(T, \{\lambda, \gamma\}) = P_{\rm HG}(T, \{\lambda, \gamma\})\,, \tag{1}$$
$$n_{B_{\rm QGP}}(T, \{\lambda, \gamma\}) = x n_{B_{\rm HG}}(T, \{\lambda, \gamma\})\,, \tag{2}$$
$$n_{Q_{\rm QGP}}(T, \{\lambda, \gamma\}) = x n_{Q_{\rm HG}}(T, \{\lambda, \gamma\})\,, \tag{3}$$
$$n_{S_{\rm QGP}}(T, \{\lambda, \gamma\}) = x n_{S_{\rm HG}}(T, \{\lambda, \gamma\})\,, \tag{4}$$
$$n_{B_{\rm QGP}}(T, \{\lambda, \gamma\}) = 2\beta n_{Q_{\rm QGP}}(T, \{\lambda, \gamma\})\,, \tag{5}$$
$$n_{S_{\rm QGP}}(T, \{\lambda, \gamma\}) = 0\,, \tag{6}$$

where the n denote the densities. For isospin symmetric systems one has to set $\beta = 1$ in (5). Equations (1)–(6) only have one free variable, necessary to produce a whole transition line in the phase diagram. At crossover, we have $x = 1$, whereas at the first order transition line the inequality $V_{\rm QGP} \neq V_{\rm HG}$ preserves the survival of x as an extra variable.

3 A solution for the transition curve

The above considerations are applicable to every partition function connected to the hadronic and the quark state. It is interesting, though, to check whether they can produce a real solution for the transition curve, i.e. that the system of (1)–(6) is not impossible. For this reason, two simple models will be employed. For the hadron gas phase only the repulsive part of the hadronic interaction will be taken into account through a Van der Waals treatment of the system volume. In order to have a thermodynamically consistent description, the grand canonical partition function of a system containing h hadronic species, each of which is associated with the chemical potential μ_i, may be written down in the form [28, 29]

$$Z_{\rm HG}(T, \{\mu\}, V) = \sum_{N_1=0}^{\infty} \cdots \sum_{N_h=0}^{\infty} \prod_{i=1}^{h} \exp\left(\frac{\mu_i N_i}{T}\right) \times Z_i^{\rm pt}(T, N_i, \hat{V})\theta(\hat{V})\,. \tag{7}$$

In (7) 'pt' refers to the ideal system of point particles, i.e. to the absence of repulsive interactions. The available volume is $\hat{V} \equiv V - \sum_{i=1}^{h} v_i N_i$, where v_i is the proper volume of the i species and N_i the number of i particles present in the system. The θ function preserves the partition function from negative contributions of the volume and is dealt with by a Laplace transformation, which causes the pressure to

acquire the form

$$P_{\rm HG}(T,\{\mu\}) = P^{\rm pt}_{\rm HG}(T,\{\tilde{\mu}\}) = \sum_{i=1}^{h} P^{\rm pt}_i(T,\tilde{\mu}_i)\,, \qquad (8)$$

where the quantities $\tilde{\mu}_i$ are connected to the chemical potentials μ_i and the system pressure

$$\tilde{\mu}_i = \mu_i - v_i P_{\rm HG}(T,\{\mu\})\,. \qquad (9)$$

In the following the Boltzmann approximation will be used. Also, the proper volumes of all the particle species will be taken equal, so

$$v_1 = \cdots = v_h = v_0\,. \qquad (10)$$

The need for these two simplifications will become apparent in Sect. 5, where the experimental data will be addressed. The ideal partition function of the point particles i is then

$$\begin{aligned}\ln Z^{\rm pt}_i(T,\mu_i,V) &= \exp\left(\frac{\mu_i}{T}\right) V \frac{T}{2\pi^2} g_i m_i^2 K_2\left(\frac{m_i}{T}\right)\\ &\equiv \exp\left(\frac{\mu_i}{T}\right) V c(T)\,, \end{aligned} \qquad (11)$$

where the g_i are degeneracy factors due to spin and isospin, and K_2 is the modified Bessel function of the second kind. The pressure of the particles of i species will then be

$$P^{\rm pt}_i(T,\mu_i) = T\frac{\ln Z^{\rm pt}_i(T,\mu_i,V)}{V} = T\exp\left(\frac{\mu_i}{T}\right) c(T)\,. \qquad (12)$$

With the use of (9), (10) and (12) it is found that

$$P^{\rm pt}_i(T,\tilde{\mu}_i) = \exp\left(-\frac{v_0 P_{\rm HG}}{T}\right) P^{\rm pt}_i(T,\mu_i)\,, \qquad (13)$$

a relation that can be inserted into (8) to give

$$P_{\rm HG}(T,\{\mu\}) = \exp\left[-\frac{v_0 P_{\rm HG}(T,\{\mu\})}{T}\right] \sum_{i=1}^{h} P^{\rm pt}_i(T,\mu_i)\,. \qquad (14)$$

Then the particular density $n_{i,\rm HG}$ can be calculated from (14) as

$$n_{i,\rm HG}(T,\{\mu\}) = \left.\frac{\partial P_{\rm HG}(T,\{\mu\})}{\partial \mu_i}\right|_{T,\mu_1,\cdots,\mu_{i-1},\mu_{i+1},\cdots,\mu_h}\,. \qquad (15)$$

Also (11) gives

$$n^{\rm pt}_i(T,\{\mu\}) = \frac{1}{T} P^{\rm pt}_i(T,\{\mu\})\,. \qquad (16)$$

Equations (14)–(16) lead to the determination of the density:

$$n_{i,\rm HG}(T,\{\mu\}) = \frac{\exp\left[-\frac{v_0 P_{\rm HG}(T,\{\mu\})}{T}\right] n^{\rm pt}_i(T,\{\mu\})}{1 + v_0 \exp\left[-\frac{v_0 P_{\rm HG}(T,\{\mu\})}{T}\right] \sum_l n^{\rm pt}_l(T,\{\mu\})}\,, \qquad (17)$$

where the summation over index l spans over all particle species.

The hadronic partition function to be used extends to all hadronic states containing u, d and s quarks as they are listed in [30]. An equivalent description is possible if the fugacities are used in place of the chemical potentials. Also the different hadrons, described in the preceding equations with index i, can be organised in families each of which is characterised by the same fugacity and contains a number of particle species differing in mass and degeneracy factors. The HG partition function for the point particles, which contains all the particle species can, in accordance to (11), be written down as follows:

$$\ln Z^{\rm pt}_{\rm HG}(V,T,\{\lambda,\gamma\}) = \frac{VT}{2\pi^2} \sum_a \lambda_a \sum_k g_{ak} m_{ak}^2 K_2\left(\frac{m_{ak}}{T}\right), \qquad (18)$$

where the g_{ak} are degeneracy factors due to spin and isospin. The index a runs over all hadronic families, each of which contains members with the same quark content, and k runs over all the particles of this family. The fugacity $\lambda_a = \prod_\nu \lambda_\nu^{N_\nu - N_{\bar\nu}} \gamma_\nu^{N_\nu + N_{\bar\nu}}$, where $\nu = u, d, s$ and $N_\nu(N_{\bar\nu})$ is the number of $\nu(\bar\nu)$ quarks contained in a hadron belonging to the family labeled a. For the light unflavoured mesons with quark content $(c_1/2)(u\bar{u} + d\bar{d}) + c_2 s\bar{s}$, $c_1 + c_2 = 1$, the fugacity used is $\lambda_a = (\gamma_u\gamma_d)^{c_1}\gamma_s^{2c_2}$. The ideal partition function (18) can be used to determine the pressure and densities of the point particle system. Thus (14) acquires the form

$$\begin{aligned} P_{\rm HG}(T,\{\lambda,\gamma\}) &= \exp\left[-\frac{v_0 P_{\rm HG}(T,\{\lambda,\gamma\})}{T}\right]\\ &\quad\times \frac{T^2}{2\pi^2} \sum_a \lambda_a \sum_k g_{ak} m_{ak}^2 K_2\left(\frac{m_{ak}}{T}\right), \end{aligned} \qquad (19)$$

which can be solved through an arithmetic procedure to evaluate the system pressure $P_{\rm HG}$ for given set of variables $(T,\{\lambda,\gamma\})$. A particular density $n^{\rm pt}_i$ can also be evaluated by (18), and using the already calculated $P_{\rm HG}$ the density with the Van der Waals corrections is

$$\begin{aligned} &n_{i,\rm HG}\,(T,\{\lambda,\gamma\})\\ &= \left(\exp\left[-\frac{v_0 P_{\rm HG}(T,\{\lambda,\gamma\})}{T}\right] n^{\rm pt}_i(T,\{\lambda,\gamma\})\right)\\ &\quad\Bigg/\left(1 + v_0 \exp\left[-\frac{v_0 P_{\rm HG}(T,\{\lambda,\gamma\})}{T}\right]\frac{T}{2\pi^2}\right.\\ &\qquad\left.\times \sum_a \lambda_a \sum_k g_{ak} m_{ak}^2 K_2\left(\frac{m_{ak}}{T}\right)\right)\\ &\equiv f(v_0;T,\{\lambda,\gamma\}) n^{\rm pt}_i(T,\{\lambda,\gamma\})\,. \end{aligned} \qquad (20)$$

For the QGP phase a simple model containing three flavours is used. The quarks are non-interacting, and only the presence of gluons is accounted for, as well as the effect of the vacuum through the MIT bag constant, B. A wealth

of quark fugacities is easily accommodated, though, in this model. The QGP partition function is consequently

$$\ln Z_{\rm QGP}(V,T,\{\lambda,\gamma\}) = \frac{N_s N_c V}{6\pi^2 T} \times \sum_\nu \int_0^\infty \frac{p^4}{\sqrt{p^2+m_j^2}} \frac{1}{\mathrm{e}^{\sqrt{p^2+m_j^2}/T}(\lambda_\nu\gamma_\nu)^{-1}+1}\,\mathrm{d}p + V\frac{8\pi^2T^3}{45} - \frac{BV}{T}\,, \quad (21)$$

where $N_s = 2$ and $N_c = 3$. The index ν runs over all quarks and antiquarks and the fugacity $\lambda_{\bar\nu} = \lambda_\nu^{-1}$ and $\gamma_{\bar\nu} = \gamma_\nu$. The current quark masses are $m_u = 1.5$, $m_d = 6.75$ and $m_s = 117.5$ MeV [30].

At the first order QGP–HG transition a mixed phase is assumed. This phase spans over a curve in the $(T,\{\lambda,\gamma\})$-space, so these variables are kept constant throughout the mixed phase. The only thermodynamic variable that is allowed to change is the system volume V. The volume equals $V_{\rm HG}$ at the pure hadronic phase, at one end of the first order transition, and $V_{\rm QGP}$ at the pure quark phase, at the other end of the transition. The system volume V of the mixed phase can then be expressed as

$$V_{\rm mixed} = \delta V_{\rm HG} + (1-\delta)V_{\rm QGP}\,. \quad (22)$$

The parameter δ is $0 \le \delta \le 1$, and for $\delta = 1$ ($\delta = 0$) we have a pure HG (QGP) phase. The mixed phase is realised in a composition of volume $\delta V_{\rm HG}$ existing in the hadronic phase and volume $(1-\delta)V_{\rm QGP}$ in the QGP phase.

The pressure of the hadronic part of the mixed system can be calculated from (19) for the hadronic volume $\delta V_{\rm HG}$. It is easily seen, though, that this pressure does not depend on the volume. Since the hadronic pressure depends only on the variables $(T,\{\lambda,\gamma\})$, which are held constant for all values of δ in (22), it is concluded that this pressure remains unchanged at every point of the mixed phase and equals $P_{\rm HG}$ of the pure hadronic phase (for $\delta = 1$). It is, also, realised by checking (21) that the QGP pressure does not depend on the volume, either. With similar reasoning, it is deduced that the pressure of the quark part of the mixed phase remains constant and equals the pressure $P_{\rm QGP}$ of the pure QGP phase (for $\delta = 0$). Then (1) ensures the equality between the pressures of the pure phases, so the pressures of the hadronic and the quark part of the mixed phase are equal. Thus

$$P_{\rm mixed} = P_{\rm HG} = P_{\rm QGP}\,. \quad (23)$$

The pressure is, consequently, kept constant throughout the first order transition. The part of the P–V isotherm that corresponds to the mixed phase is parallel to the V axis, as it is expected in a first order transition.

On the contrary, the densities vary. Equation (20) ensures that the density of the hadronic part of the mixed phase is held equal to the respective density of the pure hadronic phase, $n_{i,\rm HG}$. Equation (21) ensures that the density of the quark part of the mixed phase is held equal to the respective density of the pure quark phase, $n_{i,\rm QGP}$. But in general $n_{i,\rm HG}(T,\{\lambda,\gamma\}) \neq n_{i,\rm QGP}(T,\{\lambda,\gamma\})$. If the density n_i is associated with the quantity N_i, then

$$n_{i,\rm mixed} = \frac{N_{i,\rm mixed}}{V_{\rm mixed}} = \frac{N_{i,\rm HG}+N_{i,\rm QGP}}{V_{\rm mixed}} = \frac{\delta V_{\rm HG}}{V_{\rm mixed}} n_{i,\rm HG} + \frac{(1-\delta)V_{\rm QGP}}{V_{\rm mixed}} n_{i,\rm QGP}\,. \quad (24)$$

It is easily checked that for $\delta = 1$ ($\delta = 0$) the density of the pure hadronic (quark) state is produced. The conservation of the quantum quantities B, Q and S is ensured in the mixed phase. Equation (2) implies that $\langle B\rangle_{\rm HG} = \langle B\rangle_{\rm QGP}$. Then multiplication of both sides of (24) by $V_{\rm mixed}$ gives

$$V_{\rm mixed} n_{B\rm mixed} = \delta\langle B\rangle_{\rm HG} + (1-\delta)\langle B\rangle_{\rm QGP} \Rightarrow \langle B\rangle_{\rm mixed} = \langle B\rangle_{\rm HG} = \langle B\rangle_{\rm QGP}\,. \quad (25)$$

Equations (3) and (4) produce similar equations for Q and S.

Between the crossover region (where $x = 1$) and the first order transition line (where $x \neq 1$), the critical point resides. Observing (1)–(6), it is clear that they do not provide a restriction on x, other than that it should be a continuous function. So these equations can accommodate an additional constraint in the form of x, which may be provided by a sophisticated partition function that records the full part of the interaction (the attractive part as well).

The system of (1)–(6) can then be solved for $x = 1$ for the crossover region or for $x \neq 1$ for the first order transition curve. The system is simplified observing that the strangeness neutrality at the QGP phase (6) leads to the solution $\lambda_s = 1$. This solution is valid for every case of QGP partition function, as long as products of the fugacities of the strange quark with the fugacities of the u and d quarks do not appear. The initial system then is reduced to the system of (1)–(5) for $\lambda_s = 1$. The HG partition function (7) and the QGP partition function (21) is used for the system of (1)–(5). For the particular choices of partition functions, two parameters, B and v_0, are left open, producing different solutions for the transition curves. The system of (1)–(5) for $\lambda_s = 1$ accepts as solution for the variable γ_s the value 0, since then (4) is automatically satisfied. This is a trivial solution, because it is equivalent to the absence of the strange quarks in the system, and therefore such solutions should be excluded. Non-trivial solutions for the thermodynamic variables are depicted for $B^{1/4} = 272$ MeV in Figs. 1–4 for the isospin symmetric case ($\beta = 1$). Since the solutions are calculated in the Boltzmann approximation, which does not include any Bose singularities, additional checks are carried out for every part of the calculations to ensure that the evaluated variables are such that no Bose singularity is approached. Lines (a) represent the solution without the inclusion of pentaquarks and are drawn for $v_0 = 2.83\times10^{-8}\,\mathrm{MeV}^{-3}$. The crossover region, which is determined uniquely after setting the parameters B and v_0, is drawn everywhere with slashed lines.

Two additional issues concerning the phase transition are the position of the critical point where the cross-over region ends and the first order transition sets in, as well as the ratio of the volumes $x = V_{\rm HG}/V_{\rm QGP}$ at the first order

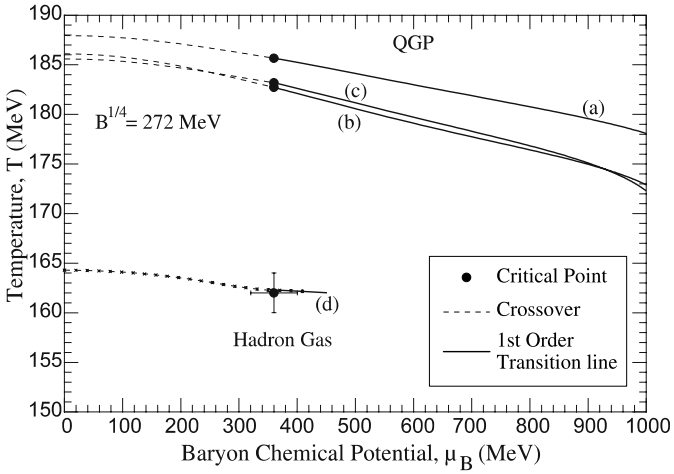

Fig. 1. Temperature as a function of chemical potential of the baryon at the QGP–hadron gas transition line for $B^{1/4} = 272\,\mathrm{MeV}$, without (lines (a),(c)) and with (line (b)) the inclusion of the pentaquark states. Lines (a) and (b) are calculated with $v_0 = 2.83 \times 10^{-8}\,\mathrm{MeV}^{-3}$ and line (c) with $v_0 = 2.06 \times 10^{-8}\,\mathrm{MeV}^{-3}$. Line (d) is the phase transition curve calculated from lattice QCD in [31]

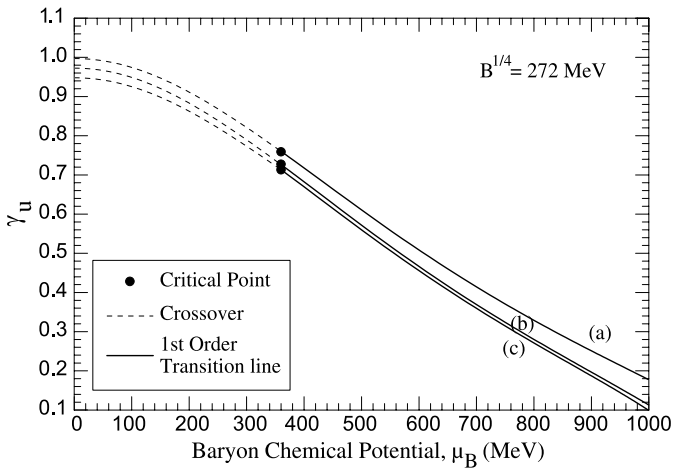

Fig. 2. Relative chemical equilibrium variable of the u quark, γ_u, as a function of the chemical potential of the baryon at the QGP–hadron gas transition line. Lines (a)–(c) correspond to lines (a)–(c) of Fig. 1

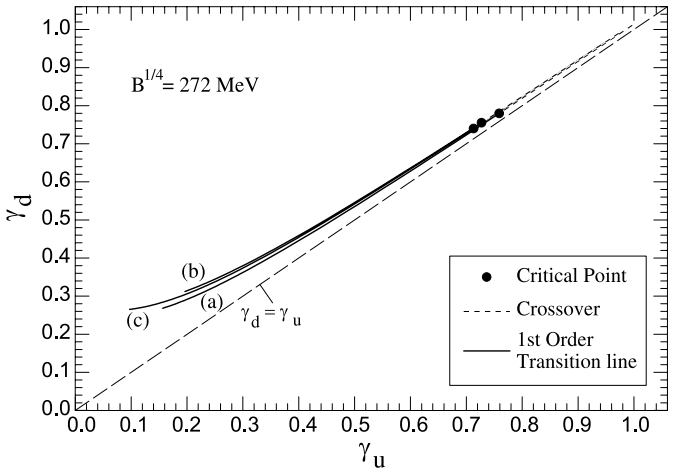

Fig. 3. Relative chemical equilibrium variable of the d quark, γ_d, as a function of the relative chemical equilibrium variable of the u quark, γ_u, at the QGP–hadron gas transition line for the isospin symmetric case. Lines (a)–(c) correspond to lines (a)–(c) of Fig. 1. The line $\gamma_d = \gamma_u$ is also depicted

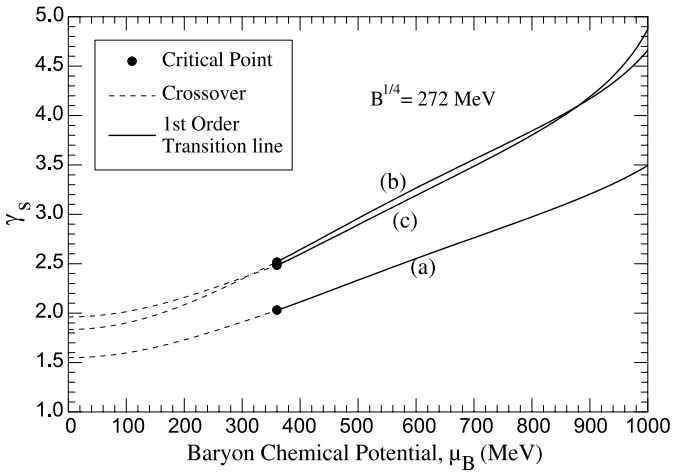

Fig. 4. Relative chemical equilibrium variable of the s quark, γ_s, as a function of the chemical potential of the baryon at the QGP–hadron gas transition line. Lines (a)–(c) correspond to lines (a)–(c) of Fig. 1

transition line. These two issues cannot be dealt with by the simple choices of partition functions used for the calculations of this section, since the attractive part of the interaction among hadrons or quarks is completely neglected. To display certain solutions for the critical curve within the context of the partition functions (7) and (21), the position for the critical point has to be chosen. However, the position of the critical point has not been well established by the various models used for its calculation. In [31], the critical point is set at $T = 162 \pm 2\,\mathrm{MeV}$, $\mu_B = 360 \pm 40\,\mathrm{MeV}$ (displayed in Fig. 1, line (d)). This position is determined by lattice QCD calculations by means of a reweightening technique using three quark flavours and considerably reduced light quark masses, approaching their physical values. In [32], with the use of two flavours of quarks and a Taylor expansion of the baryon number susceptibility, the critical point is set at lower values of μ_B ($\mu_B/T \simeq 1.1$). In [33], the position of the critical point is limited within a region in the T–μ_B plane using the statistical bootstrap. In [34] a review of our understanding of the position of the critical point in various models can be found. It should be noted that the various calculations [31–33] are carried out assuming full chemical equilibrium ($\{\gamma\} = \{1\}$) and, thus, cannot be applied to the present situation, where partial chemical equilibrium is assumed. In order to display a solution for the transition curve, the chemical potential of the baryon at the critical point is chosen as $\mu_{B,\mathrm{cr.p.}} = 360\,\mathrm{MeV}$ in Figs. 1–5. This

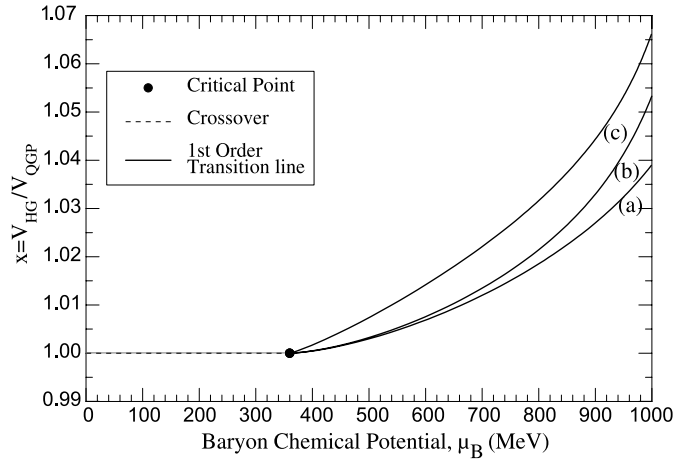

Fig. 5. Volume expansion ratio $x = V_{\rm HG}/V_{\rm QGP}$ between pure hadron and pure QGP phase at the same transition point, as a function of the chemical potential of the baryon, which was used in the calculations in Figs. 1–4. Lines (a)–(c) correspond to lines (a)–(c) of Fig. 1. In lines (a) and (b) $x_1 = 1.06$ at $\lambda_{u1} = 14.2$ and $\epsilon = 1.5$ and in line (c) $x_1 = 1.07$ at $\lambda_{u1} = 14.2$ and $\epsilon = 1.15$

choice does not present a preferable value, and any other choice can be accommodated in the set of (1)–(6).

A form for the ratio of the volumes x has to be defined as well. This form has to produce $x = 1$ at the critical point. Moreover, it is chosen to produce a given value x_1 at a specific value of λ_{u1}. A simple form that implements these demands is

$$x = 1 + \left(\frac{\ln \lambda_u - \ln \lambda_{u,\rm cr.p.}}{\ln \lambda_{u1} - \ln \lambda_{u,\rm cr.p.}} \right)^{\epsilon} (x_1 - 1)\,, \qquad (26)$$

where the exponent ϵ regulates the curvature of the first order transition line. For lines (a), $x_1 = 1.06$ at $\lambda_{u1} = 14.2$ and $\epsilon = 1.5$ are chosen. Of course, any function of x can be used, producing different first order transition curves. The resulting first order transition lines are drawn with solid lines in Figs. 1–4, while the respective critical points are represented by solid circles.

The temperature T is displayed as a function of the chemical potential of the baryon μ_B in Fig. 1. In the same figure, line (d), which represents the phase transition line as it is calculated from the lattice QCD in [31], is drawn for comparison.

The relative chemical equilibrium fugacity γ_u is displayed as a function of μ_B in Fig. 2. This particular solution leads to the gradual suppression of γ_u as the chemical potential of the baryon increases. The connection of γ_u and γ_d, for the isospin symmetric solution, is depicted in Fig. 3. The line $\gamma_u = \gamma_d$ is also drawn for comparison. The relative chemical equilibrium factor γ_s is drawn as a function of the chemical potential of the baryon in Fig. 4.

In Fig. 5 the ratios of the volumes x, which are used in the first order transition, are drawn against the chemical potential of the baryon. The forms used for x are increasing functions with respect to the chemical potential of the baryon. The resulting first order transition lines produce lower temperatures as the chemical potential of the baryon increases, something which is expected.

One direct consequence of the simultaneous solution of (1)–(6) is that the relative chemical equilibrium fugacities have values that depend on each other at every transition point. This is easily realised by inspecting the condition $n_{S_{\rm HG}} = 0$ (for $\lambda_s = 1$). The solution of this condition in the Boltzmann approximation is simplified by the assumption that isospin symmetry leads to the approximate solution $\lambda_u = \lambda_d \equiv \lambda_q$ and $\gamma_u = \gamma_d \equiv \gamma_q$. Neglecting trivial solutions, where $\gamma_s = 0$, the zero strangeness condition can be solved to give

$$\gamma_s = \frac{F_K(T) - F_H(T)\gamma_q(\lambda_q + \lambda_q^{-1})}{2F_\Xi(T)}\,. \qquad (27)$$

In (27), F_K corresponds to the kaon mesons, F_H to the hyperon baryons (Λs and Σs) and F_Ξ to the Ξ baryons, while the summation

$$F_a(T) = \frac{T}{2\pi^2} \sum_i g_{ai} m_{ai}^2 K_2 \left(\frac{m_{ai}}{T} \right) \qquad (28)$$

over all particles i of the same family is implied. In the above relation, K denotes the modified Bessel function of the second kind. It is evident from (27) that the increase of the relative chemical equilibrium factor for the light quarks, γ_q, and the increase of the light quark fugacity, λ_q, leads, at constant temperature, to a decrease of the factor γ_s.

It should be noted that the lattice QCD line (d) in Fig. 1 is calculated for $\gamma_u = \gamma_d = \gamma_s = 1$, whereas (a) is a curve in a multidimensional space. In that sense Figs. 1–4 depict the projections of the transitions curves on the corresponding 2-dimensional planes. The position where the transition line (a) intersects with the temperature axis, T_0, in Fig. 1, depends on the values of the unknown parameters B and v_0. T_0 corresponds to $\mu_u = \mu_d = \mu_s = 0$ and mainly depends on B and to a lesser extent on v_0. T_0 is found to increase if B increases for v_0 kept constant and, also, T_0 increases if v_0 increases while B remains constant. Figure 6 includes calculations without pentaquarks of T_0 for a fixed value of $v_0 = 2.83 \times 10^{-8}\,{\rm MeV}^{-3}$ and varying values of B. As B increases, while v_0 is kept constant, T_0 is driven to greater values, but at the same time all the fugacities $\{\gamma\}$ are suppressed. In Fig. 6 T_0 is plotted against the corresponding γ_u (line (1)), γ_d (line (2)) and γ_s (line (3)). The values of γ_u or γ_d are shown at the low horizontal axis and the γ_s values at the upper horizontal axis. It is clear that the increase of the pressure and the densities of the hadron gas that is due to the increase of the temperature is compensated through a reduction that is due to the suppression of $\{\gamma\}$.

In Fig. 7 the entropy to baryon number ratio (S/B) is plotted for the values of the thermodynamical variables of the transition curves (a) of Figs. 1–4. The upper line corresponds to the pure QGP phase and the lower one to the pure hadronic phase. The part related to the first order section of the transition ($\mu_B > 360\,{\rm MeV}$) is consistent with the transition from a higher entropy phase (QGP phase) to the lower entropy hadronic phase. However, the simple models

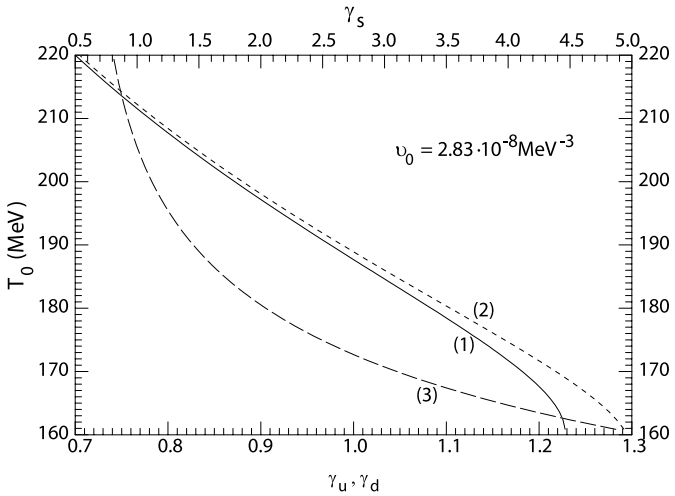

Fig. 6. Transition temperature T_0 for $\mu_u = \mu_d = \mu_s = 0$ as a function of corresponding γ_u (line (1), low axis), γ_d (line (2), low axis) and γ_s (line (3), upper axis) for $v_0 = 2.83 \times 10^{-8}$ MeV^{-3} and varying values of B (B increases as T_0 increases)

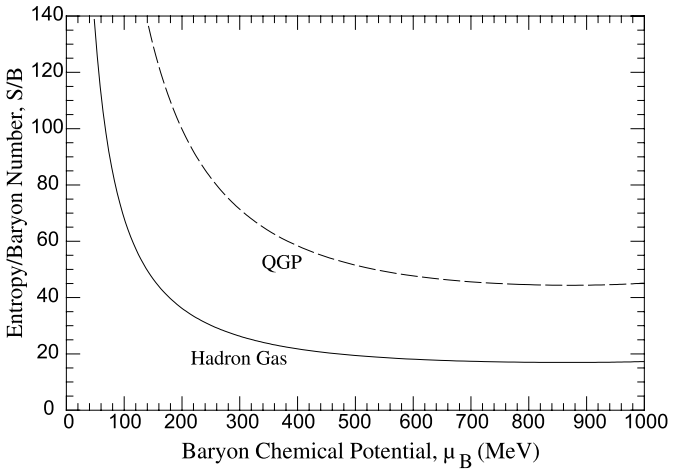

Fig. 7. The entropy to baryon number ratio calculated for the thermodynamic variables of the transition line (a) depicted on Figs. 1–5. The continuous line corresponds to the pure hadronic phase and the slashed one to the pure QGP phase

used in the calculation cannot produce the continuity of the entropy (which is related to the T-derivative of the partition function) at the crossover region ($\mu_B < 360$ MeV). The inclusion of the interaction in the quark–gluon partition function is crucial for producing a reduction of the entropy of the ideal QGP phase, and thus for having a smooth transition to the entropy of the hadron gas.

4 Inclusion of pentaquarks

Evidence has accumulated for hadrons containing five quarks. These 5-quark states are the $\Theta^+(1540)$ [35–39], with $I = 0$ and quark content $uudd\bar{s}$, and the $\Xi^*(1862)$, with $I = 3/2$. The content of the states $\Xi^*(1862)$ is $ssdd\bar{u}$ (for the state with electric charge $Q = -2$), $ssud\bar{u}$ (with $Q = -1$), $ssdd\bar{d}$ (with $Q = 0$) and $ssuu\bar{d}$ (with $Q = +1$). The existence of the first three of the states $\Xi^*(1862)$ has been confirmed [40, 41]. The motivation to investigate the effect of the pentaquark states comes from the fact that these states can alter (1)–(6), since they introduce additional hadronic families, each of which is accompanied by completely different functions between the fugacities of the system compared to the ones in the already known families. This can be easily realised if the corresponding equation of (27) is written down as follows:

$$\gamma_s = \left[F_K(T) + F_\Theta(T)\gamma_q^3\left(\lambda_q^2 + \lambda_q^{-2}\right)\left(\lambda_q + \lambda_q^{-1}\right) - F_H(T)\gamma_q\left(\lambda_q + \lambda_q^{-1}\right)\right]\left\{2\left[F_\Xi(T) + F_{\Xi^*}(T)\gamma_q^2\right]\right\}^{-1}. \quad (29)$$

The existence of the Θ hadron drives γ_s to higher values with a strong dependence on γ_q and λ_q, whereas the inclusion of the Ξ^* states contributes to the decrease of γ_s.

The system of (1)–(6) is then solved with the inclusion of the $\Theta^+(1540)$ and $\Xi^*(1862)$ states with the same partition functions for the HG and the QGP phase and for the same parameters B, v_0 as in the case without the inclusion of the pentaquarks (lines (a) of the previous section). The resulting curves are lines (b), shown in Figs. 1–4. The adopted form of the ratio of volumes x again produces the value $x_1 = 1.06$ at $\lambda_{u1} = 14.2$ (while $\epsilon = 1.5$) and is plotted in Fig. 5.

Lines (a) and (b) record the difference induced in the transition curve by the inclusion of the pentaquarks, if parameters B and v_0 remain the same and x acquires the same value at a given value of λ_u. However, none of these parameters is known, and so the difference in the transition curve cannot provide evidence for the existence of pentaquarks. For this reason lines (c) are drawn in Figs. 1–4. These lines represent a solution for the transition curve without the inclusion of the pentaquarks but for a different choice of parameters (B remains the same, $v_0 = 2.06 \times 10^{-8}$ MeV^{-3}, $x_1 = 1.07$ at $\lambda_{u1} = 14.2$ and $\epsilon = 1.15$). It is evident, now, that lines (b) (with pentaquarks included) and lines (c) (without pentaquarks) almost coincide.

5 Application to heavy-ion data

The fact that the transition territory between the hadronic and the QGP phase is restricted to a line in the space of temperature and chemical potentials produces a direct connection between the variables after the phase transition and the corresponding ones before: they *must coincide*. This is not the case when the transition territory is allowed to occupy a surface. Then the connection between the thermodynamic variables of the hadronic and the quark phase is broken. The system, as it crosses the transition territory to enter the state of hadrons, loses its "memory" of the plasma state.

In a system in which the hadronic state carries the memory of its preceding state, one may use the freeze-out

variables as a diagnostic tool for a primordial QGP phase. Two assumptions are made at this point: (i) a quark–gluon phase *has* been formed in a collision experiment, and (ii) the chemical freeze-out occurs right after the transition to the hadronic phase.

If assumptions (i) and (ii) are valid, then the freeze-out thermodynamic variables have to fulfill the constraints (1)–(6). If, on the contrary, either (i) or (ii) does not take place, then the restriction on the freeze-out conditions of the system is diminished only to

$$n_{B_{\rm HG}}(T,\{\lambda,\gamma\}) = 2\beta n_{Q_{\rm HG}}(T,\{\lambda,\gamma\})\,, \tag{30}$$
$$n_{S_{\rm HG}}(T,\{\lambda,\gamma\}) = 0\,, \tag{31}$$

a set of constraints that will be referred to from now on as set A.

The thermodynamic variables are extracted through a fit of the experimentally measured particle multiplicities or ratios to a statistical model. Such a technique has been successful. If now the additional constraints (1)–(6) are imposed, the question that arises is whether a successful fit is also produced or the restrictions that these constraints imply are inconsistent with the data.

These ideas will now be used to analyse the freeze-out variables of four heavy-ion experiments. The application of (1)–(6) requires knowledge of the partition functions for the hadron and the quark phase. The particular functions used in Sects. 3 and 4 to demonstrate the existence of a solution include the arbitrariness in the choice of the parameters B, v_0 and the quantity x. Since it is unwanted for the extracted variables to depend on the choice of unknown parameters, it is better to form and apply a subset of constraints that are completely independent from these parameters.

When the system of (1)–(6) is valid, (3)–(6) can equivalently be rewritten as

$$n_{B_{\rm HG}}(T,\{\lambda,\gamma\}) = 2\beta n_{Q_{\rm HG}}(T,\{\lambda,\gamma\})\,, \tag{32}$$
$$n_{B_{\rm QGP}}(T,\{\lambda,\gamma\}) = 2\beta n_{Q_{\rm QGP}}(T,\{\lambda,\gamma\})\,, \tag{33}$$
$$n_{S_{\rm HG}}(T,\{\lambda,\gamma\}) = 0\,, \tag{34}$$
$$n_{S_{\rm QGP}}(T,\{\lambda,\gamma\}) = 0\,. \tag{35}$$

Equation (32) results from (2), (3) and (5), whereas (34) is due to (4) and (6). For the particular model [28, 29], which has been used to include the Van der Waals volume corrections, the only way for (32) and (34) not to depend on the unknown hadronic proper volumes is to use the Boltzmann approximation and to set all the volumes equal to the same parameter v_0. Then the hadronic densities may acquire the form of (20). The function f, which is the only term in which v_0 is present, then cancels from (32) and (34). Equations (32)–(35) (referred to as set B) now form a set of equations that do not depend on the parameters v_0 for the particle size, B (MIT bag constant) nor on the ratio x applicable to the first order transition line. It is easily checked that the same is true for the set of (30)–(31), forming set A.

Equation (35) deserves special attention, since it is easily solved to give $\lambda_s = 1$. Indeed in [42, 43] lattice calculations have been carried out to evaluate the quantum number susceptibility,

$$C_{\rm BS} = 1 + 2C_{(us)/s} = 1 + \frac{1}{\chi_s}\frac{T}{V}\frac{\partial^2 \ln Z}{\partial\mu_u \partial\mu_s} = 1 + \frac{1}{\chi_s}\frac{\lambda_u\lambda_s}{V}\frac{\partial^2 \ln Z}{\partial\lambda_u \partial\lambda_s}\,.$$

It is found that $C_{\rm BS} = 1$ immediately after the system acquires the transition temperature $T_{\rm c}$ and remains constant at the unit value for all higher temperatures. Therefore, above $T_{\rm c}$ the quantum numbers are carried out by quark-like quasiparticles. The previous equation then gives $\frac{\partial^2 \ln Z}{\partial\lambda_u \partial\lambda_s} = 0$, which in turn means that products of the fugacity λ_s with other quark flavour fugacities do not appear. This suffices to give as a solution to the zero net strangeness equation (35) $\lambda_s = 1$ for any kind of partition function that may be used in place of (21). Thus, the solution $\lambda_s = 1$, to be used in the following as part of set B, is model independent.

On the contrary, (1) and (2) are model dependent and contain unknown parameters. However, if the freeze-out parameters are determined, they can be inserted in (2) to determine v_0 (assuming that x is known), and then (1) can be used to determine B. This task serves to show that (1) and (2) have a real solution, and it contributes to the overall consistency of the technique.

In order to extract the thermodynamic variables of the chemical freeze-out conditions of heavy-ion experiments, a fitting procedure has to be carried out on the measured hadronic multiplicities. The theoretical form for the number of particles of type i, $N_i^{\rm th}$, is according to (20)

$$N_i^{\rm th} = V n_i = V f(v_0;T,\{\lambda,\gamma\}) n_i^{\rm pt}(T,\{\lambda,\gamma\})\,. \tag{36}$$

The term Vf, which includes v_0, is common, now, to all multiplicities. Thus, the ratio of every two multiplicities with volume corrections equals the ratio of the respective multiplicities calculated for the ideal case. This attribute leads to the desirable result that the extracted variables $(T,\{\lambda,\gamma\})$ do not depend on the unknown parameter v_0. This parameter only appears in the term Vf, and its knowledge is needed only if the volume V is to be evaluated. Also, it would not be so prudent to leave v_0 as an open variable to be evaluated along with the other variables as a result from the fit on the multiplicities. Since v_0 is a parameter in the description of the hadron gas, common to all cases, it would be undesirable for it to acquire different values from the fits of different experiments. This is an additional reason for the use of the Boltzmann approximation and only one parameter v_0 in the model for the volume corrections.

In the following, the freeze-out variables for the experiments S + S [44–53], S + Ag [54–60] (NA35) at beam energy 200 AGeV, Pb + Pb [61–65] (NA49) at beam energy 158 AGeV and Au + Au [66–73] (STAR) at $\sqrt{s_{NN}} =$ 130 GeV will be analysed. The data used are listed in Table 1 and they are in all cases full phase space multiplicities, except from the RHIC data, which are measured in midrapidity. The experiments to be analysed are chosen because, according to previous analyses, they do not pro-

Table 1. The full phase space multiplicities from the collision experiments S + S (NA35), S + Ag (NA35) and Pb + Pb (NA49), as well as the midrapidity multiplicities and ratios from Au + Au (STAR), used in the fits

S + S		S + Ag		Pb + Pb		Au + Au	
K^+	12.5 ± 0.4	${K_s}^0$	15.5 ± 1.5	N_p	362 ± 5.1	Λ	17.20 ± 1.75
K^-	6.9 ± 0.4	Λ	15.2 ± 1.2	K^+	103 ± 7.1	$\overline{\Lambda}$	12.15 ± 1.25
${K_s}^0$	10.5 ± 1.7	$\overline{\Lambda}$	2.6 ± 0.3	K^-	51.9 ± 3.6	Ξ^-	2.11 ± 0.23
Λ	9.4 ± 1.0	$\overline{p}$	2.0 ± 0.8	${K_s}^0$	81 ± 4	$\overline{\Xi}^+$	1.77 ± 0.19
$\overline{\Lambda}$	2.2 ± 0.4	$p - \overline{p}$	43 ± 3	ϕ	7.6 ± 1.1	$\Omega + \overline{\Omega}$	0.585 ± 0.150
$\overline{p}$	1.15 ± 0.40	$B - \overline{B}$	105 ± 12	Λ	53 ± 5	p	26.37 ± 2.60
$p - \overline{p}$	21.2 ± 1.3	$h^{-(*)}$	186 ± 11	$\overline{\Lambda}$	4.64 ± 0.32	$\overline{p}$	18.72 ± 1.90
$B - \overline{B}$	54 ± 3			Ξ^-	4.45 ± 0.22	${K_s}^0$	36.7 ± 5.5
$h^{-(*)}$	98 ± 3			$\overline{\Xi}^+$	0.83 ± 0.04	ϕ	5.73 ± 0.78
				Ω	0.62 ± 0.09	K^{*0}	10.0 ± 2.70
				$\overline{\Omega}$	0.20 ± 0.03	$\pi^{+(*)}$	239 ± 10.6
				$\pi^{+(*)}$	619 ± 35.4	$\pi^{-(*)}$	239 ± 10.6
				$\pi^{-(*)}$	639 ± 35.4	K^+/K^-	1.092 ± 0.023
						$\overline{K}^{*0}/K^{*0}$	0.92 ± 0.27
						$\overline{\Omega}/\Omega$	0.95 ± 0.16

$^{(*)}$ This multiplicity has not been used in the fits where the pions are excluded.

duce a high chemical potential of the baryon at freeze-out, and so they are probably at the crossover area, allowing one to set $x = 1$. The technique, though, can be applied to the first order transition case, determining the freeze-out variables, since the equations of set B do not depend on x, but then the parameters v_0 and B cannot be uniquely determined. Thus, all the extracted variables that will be presented, except v_0 and B, remain unchanged if the system undergoes a first or higher order transition.

The theoretical calculation of the particle multiplicity necessary to perform a fit to the experimental data has been carried out with the use of (36). The feeds from the decay of resonances have been included. The value of β is set to 1 in the case of S + S, 1.1 in the case of S + Ag, 1.27 for Pb + Pb and 1.25 for Au + Au.

In Table 2 the freeze-out variables are extracted without assumption (i) or (ii) (constraints of set A), whereas in Table 3a and b assumptions (i) and (ii) are assumed, thus applying the constraints of set B. Another issue concerning the analysis is the observation that the inclusion of the pion multiplicity deteriorates the fit [14, 15, 74].[1] Since the quality of the fitting procedure is of importance in evaluating the results, and a bad fit, when the constraints of set B are imposed, may be partly due to the presence of the multiplicity of the pion, two fits are performed in case of set B; one with all the multiplicities included (Table 3a) and one without the multiplicities that contain pions (Table 3b). This makes clear the effect of the pion multiplicities in the overall procedure.

The first observation that can be made by comparing the first and the second part of every table is that the inclusion of pentaquarks has a negligible effect on the evaluated parameters or the quality of the fit. So one can safely draw equivalent conclusions by performing the analysis with the pentaquarks or without them.

For the S + S and S + Ag data the fit with set B is of medium quality ($\chi^2/\mathrm{dof} = 2.98$ and 1.93, respectively) when the pions are present. This is not far worse, though, than the fit in the case of set A. When the pions are excluded, the fit with set B turns out to be very good ($\chi^2/\mathrm{dof} = 0.469$ and 0.0662, respectively), while the temperature remains at acceptable values, proving these cases to be completely compatible with a primordial quark–gluon phase. Another observation is that the imposition of set B with respect to set A, in every case, does not produce a dramatic change in the quality of the fit.

In the case of Pb + Pb the fit is relatively good with the imposition of set A ($\chi^2/\mathrm{dof} = 2.56$), but the imposition of set B severely worsens the quality of the fit. The situation cannot be remedied with the exclusion of pions, and χ^2/dof remains at the value of 18.0–18.2. The conclusion to be drawn from the bad quality of the fit with the imposition of the constraints of set B is that the data of this experiment are not compatible with assumptions (i) and (ii). Indeed, as it is evident from Table 3a and b, the freeze-out position of Pb + Pb is driven at $\mu_B = 701$–$776\,\mathrm{MeV}$ when set B is imposed. This is almost twice the higher value of the chemical potential of the baryon of the three other experiments. At this high density, it is not certain whether the chemical freeze-out occurs immediately after the system has crossed the transition line or at a point further inside the hadronic phase. The dramatic change in the quality of the fit between the cases of set A and B should be noted as well.

Also the freeze-out temperature in the case of set B is unrealistically high and rises enormously with respect to the

[1] The presence of excess of pions, though, can be connected with a primordial high entropy phase or with a phase with the chiral symmetry restored [75, 76].

Table 2. The results of fits on the S + S (NA35), S + Ag (NA35), Pb + Pb (NA49) and Au + Au (STAR) data with the imposition of the set of constraints A, without and with the inclusion of the pentaquark states. In the fits all the multiplicities have been included. The fits on the STAR data have been performed with the temperature held fixed at the given value using Bose or Fermi statistics.

	set A, fit with all			
	S + S	S + Ag	Pb + Pb	Au + Au
No pentaquarks				
χ^2/dof	$6.18/3 = 2.06$	$4.23/1 = 4.23$	$17.90/7 = 2.56$	$8.96/9 = 0.996$
T (MeV)	207 ± 26	238 ± 42	196 ± 13	154(fixed)
λ_u	1.78 ± 0.14	1.78 ± 0.18	1.729 ± 0.058	1.081 ± 0.011
λ_d	1.325 ± 0.053	1.464 ± 0.095	1.639 ± 0.041	1.0657 ± 0.0094
λ_s	1.016 ± 0.028	1.018 ± 0.028	1.166 ± 0.011	1.0190 ± 0.0035
γ_u	0.54 ± 0.16	0.45 ± 0.15	0.431 ± 0.080	1.065 ± 0.082
γ_d	1.05 ± 0.23	0.68 ± 0.21	0.565 ± 0.090	1.77 ± 0.23
γ_s	0.50 ± 0.12	0.332 ± 0.087	0.364 ± 0.062	1.427 ± 0.078
VfT^3	177 ± 33	357 ± 77	3760 ± 370	442 ± 73
μ_B (MeV)	236 ± 37	318 ± 68	301 ± 23	31.5 ± 3.2
With pentaquarks				
χ^2/dof	$6.33/3 = 2.11$	$4.16/1 = 4.16$	$17.87/7 = 2.55$	$8.99/9 = 0.999$
T (MeV)	207 ± 26	237 ± 42	196 ± 13	154(fixed)
λ_u	1.78 ± 0.13	1.78 ± 0.18	1.729 ± 0.058	1.081 ± 0.011
λ_d	1.327 ± 0.053	1.461 ± 0.094	1.638 ± 0.041	1.0660 ± 0.0094
λ_s	1.019 ± 0.028	1.021 ± 0.028	1.166 ± 0.011	1.0195 ± 0.0035
γ_u	0.54 ± 0.16	0.45 ± 0.15	0.430 ± 0.079	1.065 ± 0.083
γ_d	1.04 ± 0.23	0.69 ± 0.21	0.565 ± 0.089	1.78 ± 0.23
γ_s	0.49 ± 0.12	0.334 ± 0.088	0.364 ± 0.061	1.428 ± 0.079
VfT^3	177 ± 33	356 ± 76	3760 ± 368	441 ± 74
μ_B (MeV)	237 ± 37	317 ± 68	301 ± 23	31.7 ± 3.2

case of set A. For consistency reasons it should be recorded that a fit similar to the one presented in Table 2 for Pb + Pb has been performed in [77]. The difference in the extracted variables is due to the inclusion of the Ω and Ξ in the fit presented here. If the Ω and Ξ are excluded but the fit is carried out in the Boltzmann statistics (without the pentaquarks), the extracted variables are found to be $T = 167\,\mathrm{MeV}$, $\lambda_u = 1.71$, $\lambda_d = 1.59$, $\lambda_s = 1.19$, $\gamma_u = 0.637$, $\gamma_d = 0.901$ and $\gamma_s = 0.559$. If Bose or Fermi statistics is used in the fit without the Ω and Ξ, the freeze-out point turns out to lie close to the Bose singularity, producing then a considerable change compared to the result in Boltzmann statistics. The variables are then $T(\text{fixed}) = 140\,\mathrm{MeV}$, $\lambda_u = 1.65$, $\lambda_d = 1.65$, $\lambda_s = 1.20$, $\gamma_u = 1.48$, $\gamma_d = 1.72$ and $\gamma_s = 1.36$; these are close to the ones recorded in [77]. However, if the Ω and Ξ are excluded and also Bose or Fermi statistics is used in the fit with set B, the extracted variables have a negligible difference from the ones recorded in Table 3. The extracted variables (for the fit with all the multiplicities) are then $T = 434\,\mathrm{MeV}$, $\lambda_u = 1.71$, $\lambda_d = 1.77$, $\gamma_u = 0.269$, $\gamma_d = 0.289$ and $\gamma_s = 0.198$. Since the imposition of set B is the primary aim of this work, no reason is found for the exclusion of the multiplicities of the Ω and Ξ.

The findings concerning the S + S and S + Ag data are also in agreement with the proximity of the chemical freeze-out points of these experiments to the statistical bootstrap critical line that was found in [14, 15]. On the contrary, the freeze-out point of Pb + Pb was not found to possess such an attribute in [78], which is also in agreement with the present results.

In the case of RHIC and for set A the minimum value of χ^2 is generated for variables close to the Bose singularity.[2] This causes the differences between the results obtained with Boltzmann and Bose or Fermi statistics to increase. For this reason the results of the fit for the Au + Au case of Table 2 are presented using Bose or Fermi statistics (though (20) and (36) are valid only approximately in such a case [28, 29]). This allows for a direct comparison with similar fits, see e.g. [77], and causes no problem in the extraction of the parameters v_0 and B, because these parameters are not evaluated for the set of constraints A. Since the minimisation routine becomes rather inefficient very close to the Bose singularity, the temperature is held constant close to (but not exactly at) the value that produces the minimum χ^2, and then the rest of the vari-

[2] In [79] another result for the extracted variables for case of set A, containing a higher temperature and suppressed $\{\gamma\}$, was presented. These variables correspond to another local minimum of χ^2, which, although it produces a higher value of χ^2 than the one produced here, is away from the Bose singularity and, thus, easily accessible for the minimisation routines. This choice in [79] was made since fits with set A in the case of Au + Au mainly serve to show the reduction of the χ^2/dof value when the pions are excluded.

Table 3. The results of fits on the S + S (NA35), S + Ag (NA35), Pb + Pb (NA49) and Au + Au (STAR) data with the imposition of the set of constraints B, without and with the inclusion of the pentaquark states. In part (a) all the multiplicities have been included in the fit and in part (b) the multiplicities that contain pions have been excluded from the fit

	(a) set B, fit with all			
	S + S	S + Ag	Pb + Pb	Au + Au
No pentaquarks				
χ^2/dof	$14.9/5 = 2.98$	$5.78/3 = 1.93$	$162/9 = 18.0$	$42.3/11 = 3.85$
T (MeV)	245 ± 19	275 ± 30	436 ± 21	344 ± 15
λ_u	1.537 ± 0.025	1.613 ± 0.034	1.668 ± 0.019	1.082 ± 0.011
λ_d	1.535 ± 0.025	1.638 ± 0.036	1.728 ± 0.022	1.086 ± 0.011
γ_u	0.574 ± 0.085	0.456 ± 0.078	0.2724 ± 0.0093	0.349 ± 0.016
γ_d	0.576 ± 0.086	0.470 ± 0.080	0.293 ± 0.010	0.381 ± 0.017
γ_s	0.394 ± 0.063	0.308 ± 0.051	0.1878 ± 0.0065	0.322 ± 0.016
VfT^3	155.1 ± 5.3	282.9 ± 9.1	684 ± 33	382 ± 14
μ_B (MeV)	315 ± 26	403 ± 46	701 ± 35	84.1 ± 8.7
v_0 (10^{-8} MeV^{-3})	3.48 ± 0.66	3.48 ± 0.50	2.150 ± 0.076	2.781 ± 0.047
$B^{1/4}$ (MeV)	321 ± 23	352 ± 36	534 ± 25	431 ± 18
With pentaquarks				
χ^2/dof	$15.1/5 = 3.03$	$5.79/3 = 1.93$	$162/9 = 18.1$	$42.4/11 = 3.85$
T (MeV)	247 ± 18	277 ± 29	438 ± 21	345 ± 15
λ_u	1.537 ± 0.025	1.613 ± 0.034	1.668 ± 0.019	1.082 ± 0.011
λ_d	1.536 ± 0.025	1.638 ± 0.036	1.728 ± 0.022	1.086 ± 0.011
γ_u	0.567 ± 0.081	0.452 ± 0.076	0.2720 ± 0.0093	0.349 ± 0.016
γ_d	0.569 ± 0.082	0.466 ± 0.078	0.293 ± 0.010	0.380 ± 0.017
γ_s	0.391 ± 0.061	0.306 ± 0.050	0.1876 ± 0.0065	0.322 ± 0.016
VfT^3	151.9 ± 5.4	277.4 ± 8.6	677 ± 32	381 ± 14
μ_B (MeV)	319 ± 25	406 ± 45	704 ± 35	84.3 ± 8.7
v_0 (10^{-8} MeV^{-3})	3.57 ± 0.59	3.51 ± 0.45	2.136 ± 0.076	2.783 ± 0.046
$B^{1/4}$ (MeV)	324 ± 23	355 ± 36	536 ± 25	432 ± 18
	(b) set B, fit with no πs			
	S + S	S + Ag	Pb + Pb	Au + Au
No pentaquarks				
χ^2/dof	$1.88/4 = 0.469$	$0.132/2 = 0.0662$	$128/7 = 18.2$	$10.4/9 = 1.16$
T (MeV)	192 ± 21	207 ± 31	443 ± 25	210 ± 10
λ_u	1.603 ± 0.042	1.661 ± 0.043	1.746 ± 0.024	1.074 ± 0.010
λ_d	1.599 ± 0.042	1.693 ± 0.046	1.817 ± 0.027	1.080 ± 0.011
γ_u	0.97 ± 0.31	0.78 ± 0.31	0.261 ± 0.011	0.77 ± 0.10
γ_d	0.98 ± 0.31	0.80 ± 0.31	0.279 ± 0.011	0.83 ± 0.10
γ_s	0.87 ± 0.32	0.61 ± 0.26	0.1983 ± 0.0077	0.89 ± 0.13
VfT^3	95 ± 27	202 ± 63	626 ± 35	261 ± 27
μ_B (MeV)	271 ± 31	324 ± 50	776 ± 47	47.1 ± 5.2
v_0 (10^{-8} MeV^{-3})	3.63 ± 1.79	3.61 ± 2.14	2.068 ± 0.092	2.90 ± 0.74
$B^{1/4}$ (MeV)	271 ± 28	284 ± 41	542 ± 30	289 ± 14
With pentaquarks				
χ^2/dof	$1.53/4 = 0.383$	$0.130/2 = 0.0651$	$128/7 = 18.3$	$10.5/9 = 1.17$
T (MeV)	194 ± 18	215 ± 27	445 ± 25	213 ± 11
λ_u	1.607 ± 0.041	1.664 ± 0.044	1.746 ± 0.024	1.075 ± 0.010
λ_d	1.602 ± 0.041	1.693 ± 0.046	1.817 ± 0.027	1.080 ± 0.011
γ_u	0.97 ± 0.28	0.73 ± 0.24	0.260 ± 0.010	0.735 ± 0.091
γ_d	0.98 ± 0.28	0.75 ± 0.24	0.279 ± 0.011	0.80 ± 0.10
γ_s	0.89 ± 0.30	0.57 ± 0.20	0.1982 ± 0.0076	0.85 ± 0.12
VfT^3	90 ± 25	203 ± 54	620 ± 34	265 ± 27
μ_B (MeV)	275 ± 28	335 ± 45	780 ± 46	48.3 ± 5.3
v_0 (10^{-8} MeV^{-3})	3.98 ± 1.45	3.79 ± 1.58	2.055 ± 0.092	3.01 ± 0.72
$B^{1/4}$ (MeV)	274 ± 25	291 ± 35	544 ± 30	293 ± 14

ables are determined in order to minimise χ^2. The number of degrees of freedom, though, is recorded equal to the value that this number would acquire if no variable were held fixed during the minimisation process, aiming to have a comparison with the fits of case B, these being treated on an equal footing. The value of χ^2/dof is 0.996. Similar results are obtained when set B is imposed, but now the Boltzmann approximation proves to be efficient. The fit in the presence of pions is not of so good a quality ($\chi^2/\mathrm{dof} = 3.85$), and the temperature acquires too high a value. The fit turns out to be quite good, though, when the pions are excluded ($\chi^2/\mathrm{dof} = 1.16$), and the temperature remains at acceptable values, so the thermodynamic parameters are compatible with a QGP phase and an immediate freeze-out after the transition to the hadronic phase.

Two additional remarks are in order. The first one concerns the justification of the use of the Boltzmann approximation. In [79] similar fits were performed with the use of the Bose or Fermi statistics. In all the fits, except for Au + Au in Table 2, it is easily seen that the difference between the two statistics is small. Since the main objective is to find out whether the experiments are compatible with the set of constraints B, and the parameters v_0 and B cannot be calculated in the case of set A, no problem is caused even for the only case in which there is a considerable difference between the two statistics. The second one is that the fugacities γ_u, γ_d are in strong correlation with the temperature. During the fitting procedures, it is found that the increase of temperature is connected, in general, to the suppression of γ_u, γ_d. When the values of γ_u, γ_d are locked near the unit value, the fitted temperature is lower compared to the temperature that results from a fit in which the γ_u, γ_d acquire, through a minimisation procedure, low values.

The extracted parameters in the case of set B are inserted to (1) and (2) and the parameters v_0 and $B^{1/4}$ are also determined. In the determination of the error of v_0, the errors from all six variables $T, \lambda_u, \lambda_d, \gamma_u, \gamma_d, \gamma_s$ contribute. Especially, the error of the temperature produces a substantially higher relative error in v_0. For this reason, the recorded error of v_0 in Table 3 is calculated with half the errors of the thermodynamic variables. It is interesting that in the cases of S + S, S + Ag and Au + Au (without the pions), which have been proven to be compatible with set B, all the calculated values of v_0 and $B^{1/4}$ are close, compatible with a unique value for these parameters. On the contrary, the Pb + Pb case produces values of v_0 and $B^{1/4}$ that seem to have less connection with the rest of the cases.

The necessity of the expansion of the fugacity sector with the partial equilibrium fugacities is also revealed with the application of the present technique. If these fugacities are set to $\gamma_u = \gamma_d = \gamma_s = 1$, then the sector of the phase space that is compatible with the QGP–hadron transition is severely limited. In such a case, if a similar fit to the one with set B is performed, apart from the fact that (32) and (33) cannot be accommodated, the fit turns out to be worse. The result in the case without the pions and without pentaquarks is then $\chi^2/\mathrm{dof} = 0.605, 1.05, 27.6$ and 1.81 for S + S, S + Ag, Pb + Pb and Au + Au, respectively. Then in the case of Au + Au the compatibility with set B turns out to be dubious.

Another general observation, which can be made on Table 3, is that in the cases that are compatible with set B (S + S, S + Ag and Au + Au), the inclusion of the pions in the fits produces a dramatic increase in the value of χ^2/dof relative to the fits without the pions. This is checked by comparing the value of χ^2/dof in Table 3b and a. Although in the present work the fugacities γ_u and γ_d are used, which describe off chemical equilibrium effects, and the pion contains u and d quarks, this dramatic increase in χ^2/dof when the pions enter the fit persists. Thus, for such cases, the fugacities γ_u and γ_d cannot improve the fit to acceptable limits and reveal that an excess of pions is present.

Gathering the observations made in this section, what is found is that the freeze-out conditions of some experiments are compatible with a QGP phase and an immediate chemical freeze-out after crossing the transition line (constraints B). This is revealed by the fact that the imposition of constraints B produces fits with acceptable values of χ^2/dof and temperature. The opposite is true for the experiments incompatible with assumptions (i) or (ii). In such cases the imposition of constraints B leads to high values of χ^2/dof and temperature, though these values are acceptable when only constraints A are imposed. Also, the cases compatible with set B present an excess in the pion multiplicity that cannot properly be fitted by the γ_u and γ_d fugacities. This is seen by a great increase in the value of χ^2/dof when the pions are included in the fit in comparison to the fits without pions.

6 Conclusions

Although two different partition functions are used for the description of the quark and hadronic side of matter, it is possible to preserve the continuity of all chemical potentials and, of course, temperature and pressure (Gibbs equilibrium conditions) at the transition region, which is confined to a curve. Also, all the constraints imposed by the conservation laws of quantum quantities can be applied, leading, at the same time, to a non-trivial solution of the thermodynamic variables for a three quark flavour system. The key issue for the success of this project is the expansion of the fugacity sector of the available variables, and the relative chemical equilibrium variables already introduced can be used to serve this purpose.

Despite the fact that the space of the thermodynamic variables is extended, the restrictions imposed on the transition points produce relations among these variables. A part of these relations, in a simple form, is expressed in (27) or (29).

The restrictions on the freeze-out conditions, imposed by the existence of a quark–gluon state in the early stages after a collision experiment and a freeze-out occurring just after the phase transition, can be applied to every case in

which the thermalisation of the produced hadrons has been proven. They can serve to separate the experiments compatible with the QGP state from those that may not be. The expansion of the fugacity sector with the partial equilibrium fugacities, though, augments the part of the phase space allowed by such constraints.

The whole methodology that was presented here can be used for every grand canonical partition function adopted for the description of the HG or QGP phase. The inclusion of the interaction is crucial for the prediction of the critical point and the volume expansion ratio, which could not be determined by the models used in this work. At the moment, lattice calculations have led to the determination of the quark–gluon equation of state with three quark flavours at finite chemical potential of the baryon [31, 80]. It would be interesting, though, if these calculations could be extended with the inclusion of the relative chemical equilibrium variables for light and strange quarks, allowing for matching with the existing hadron gas models. For the hadronic side of matter the inclusion of the attractive part of interaction can be incorporated via the statistical bootstrap [12–15], in which the prediction of a critical point is also possible [33, 81, 82]. The incorporation of the full set of parameters γ_i into these studies would allow for a more precise matching with a primordial quark phase.

Acknowledgements. I would like to thank Professor J. Rafelski for fruitful discussions. I would, also, like to thank Professors N.G. Antoniou, C.N. Ktorides and F.K. Diakonos for useful remarks. This work is supported by the EPEAEK research funding program "Pythagoras I" (70/3/7315).

References

1. J. Cleymans, H. Satz, Z. Phys. C **57**, 135 (1993)
2. J. Rafelski, Phys. Lett. B **262**, 333 (1991)
3. J. Letessier, A. Tounsi, J. Rafelski, Phys. Lett. B **292**, 417 (1992)
4. C. Slotta, J. Sollfrank, U. Heinz, hep-ph/9504225
5. J. Sollfrank, M. Gaździcki, U. Heinz, J. Rafelski, Z. Phys. C **61**, 659 (1994)
6. M.N. Asprouli, A.D. Panagiotou, Phys. Rev. C **51**, 1444 (1995)
7. J. Letessier, A. Tounsi, U. Heinz, J. Sollfrank, J. Rafelski, Phys. Rev. D **51**, 3408 (1995)
8. F. Becattini, M. Gaździcki, J. Sollfrank, Eur. Phys. J. C **5**, 143 (1998)
9. J. Rafelski, J. Letessier, presented at 15th Winter Workshop on Nuclear Dynamics, Park City, UT, 9–16 January 1999, hep-ph/9902365
10. F. Becattini, M. Gaździcki, A. Keränen, J. Manninen, R. Stock, Phys. Rev. C **69**, 024 905 (2004)
11. J. Letessier, G. Torrieri, S. Steinke, J. Rafelski, Phys. Rev. C **68**, 061 901 (2003)
12. R. Hagedorn, Nuovo Cim. Suppl. **III**, 147 (1965)
13. R. Hagedorn, Nuovo Cim. Suppl. **VI**, 311 (1968)
14. A.S. Kapoyannis, C.N. Ktorides, A.D. Panagiotou, Phys. Rev. C **58**, 2879 (1998)
15. A.S. Kapoyannis, C.N. Ktorides, A.D. Panagiotou, Eur. Phys. J. C **14**, 299 (2000)
16. F. Wilczek, hep-ph/0003183
17. J. Berges, K. Rajagopal, Nucl. Phys. B **538**, 215 (1999)
18. M.A. Halasz, A.D. Jackson, R.E. Shrock, M.A. Stephanov, J.J. Verbaarschot, Phys. Rev. D **58**, 096 007 (1998)
19. J. Letessier, A. Tounsi, Nuovo Cim. A **99**, 521 (1988)
20. K. Redlich, Z. Phys. C **27**, 633 (1985)
21. K.S. Lee, M.J. Roades-Brown, U. Heinz, Phys. Lett. B **174**, 123 (1986)
22. P.R. Subramanian, H. Stöcker, W. Greiner, Phys. Lett. B **173**, 468 (1986)
23. C. Greiner, P. Koch, H. Stöcker, Phys. Rev. Lett. **58**, 1825 (1987)
24. B. Lukács, J. Zimányi, N.L. Balazs, Phys. Lett. B **183**, 27 (1987)
25. J. Cleymans, M.I. Gorenstein, J. Stalnacke, E. Suhonen, Phys. Scripta **48**, 277 (1993)
26. U. Heinz, P.R. Subramanian, H. Stöcker, W. Greiner, J. Phys. G **12**, 1237 (1986)
27. C. Greiner, H. Stöcker, Phys. Rev. D **44**, 3517 (1991)
28. D.H. Rischke, M.I. Gorenstein, H. Stöcker, W. Greiner, Z. Phys. C **51**, 485 (1991)
29. G.D. Yen, M.I. Gorenstein, W. Greiner, S.N. Yang, Phys. Rev. C **56**, 2210 (1997)
30. Particle Data Group, K. Hagiwara et al., Phys. Rev. D **66**, (2002)
31. Z. Fodor, S.D. Katz, JHEP **0404**, 050 (2004)
32. R.V. Gavai, S. Gupta, Phys. Rev. D **71**, 114 014 (2005)
33. N.G. Antoniou, F.K. Diakonos, A.S. Kapoyannis, Nucl. Phys. A **759**, 417 (2005)
34. M.A. Stephanov, Prog. Theor. Phys. Suppl. **153**, 139 (2004)
35. LEPS Collaboration, T. Nakano et al., Phys. Rev. Lett. **91**, 012 002 (2003)
36. DIANA Collaboration, V.V. Barmin et al., Phys. Atom. Nucl. **66**, 1715 (2003)
37. DIANA Collaboration, V.V. Barmin et al., Yad. Fiz. **66**, 1763 (2003)
38. CLAS Collaboration S. Stepanyan et al., Phys. Rev. Lett. **91**, 252 001 (2003)
39. SAPHIR Collaboration, J. Barth et al., hep-ex/0307083
40. NA49 Collaboration, C. Alt, et al., Phys. Rev. Lett. **92**, 042 003 (2004)
41. R. Jaffe, talk given at Quark Matter 2004, Oakland, California, January 11–17, 2004
42. R.V. Gavai, S. Gupta, Phys. Rev. D **73**, 014 004 (2006)
43. R.V. Gavai, S. Gupta, talk given at International Conference on Strangeness in Quark Matter, Los Angeles, California, March 26–31, 2006, J. Phys. G **32**, S275 (2006)
44. NA35 Collaboration, J. Bartke et al., Z. Phys. C **48**, 191 (1990)
45. NA35 Collaboration, J. Baechler et al., Nucl. Phys. A **525**, 59c (1991)
46. NA35 Collaboration, J. Baechler et al., Nucl. Phys. A **525**, 221c (1991)
47. NA35 Collaboration, J. Baechler et al., Nucl. Phys. A **544**, 293c (1992)
48. NA35 Collaboration, J. Baechler et al., Z. Phys. C **58**, 367 (1993)
49. NA35 Collaboration, T. Alber et al., preprint IKF-HENPG /6-94
50. NA35 Collaboration, J. Bächler et al., Phys. Rev. Lett. **72**, 1419 (1994)
51. NA35 Collaboration, T. Alber et al., Z. Phys. C **64**, 195 (1994)
52. NA35 Collaboration, M. Gaździcki et al., Nucl. Phys. A **566**, 503c (1994)

53. NA35 Collaboration, T. Alber et al., Phys. Lett. B **366**, 56 (1996)
54. NA35 Collaboration, J. Baechler et al., Eur. Phys. J. C **2**, 643 (1998)
55. NA35 Collaboration, J. Baechler et al., Phys. Rev. Lett. **72**, 1419 (1994)
56. NA35 Collaboration, T. Alber et al., Z. Phys. C **64**, 195 (1994)
57. NA35 Collaboration, T. Alber et al., Phys. Lett. B **366**, 56 (1996)
58. NA35 Collaboration, D. Rohrich et al., Nucl. Phys. A **566**, 35c (1994)
59. F. Becattini, J. Phys. G **23**, 1933 (1997)
60. F. Becattini, M. Gaździcki, J. Sollfrank, Eur. Phys. J. C **5**, 143 (1998)
61. NA49 Collaboration, S.V. Afanasiev et al., Phys. Rev. C **66**, 054 902 (2002)
62. S.V. Afanasiev et al., Nucl. Phys. A **715**, 161 (2003)
63. S.V. Afanasiev et al., Nucl. Phys. A **715**, 453 (2003)
64. NA49 Collaboration, S.V. Afanasev et al., Phys. Lett. B **491**, 59 (2000)
65. NA49 Collaboration, S.V. Afanasiev et al., Phys. Lett. B **538**, 275 (2002)
66. STAR Collaboration, C. Adler et al., Phys. Rev. Lett. **89**, 092 301 (2002)
67. STAR Collaboration, J. Adams et al., Phys. Rev. Lett. **92**, 182 301 (2004)
68. STAR Collaboration, J. Adams et al., Phys. Rev. C **70**, 041 901 (2004)
69. STAR Collaboration, C. Adler et al., Phys. Lett. B **595**, 143 (2004)
70. STAR Collaboration, C. Adler et al., Phys. Rev. C **65**, 041 901(R) (2002)
71. STAR Collaboration, C. Adler et al., Phys. Rev. C **66**, 061 901 (2002)
72. STAR Collaboration, J. Adams et al., nucl-ex/0311017
73. STAR Collaboration, J. Adams et al., Phys. Lett. B **567**, 167 (2003)
74. J. Sollfrank, J. Phys. G **23**, 1903 (1997)
75. J. Letessier, A. Tounsi, U. Heinz, J. Sollfrank J. Rafelski, Phys. Rev. Lett. **70**, 3530 (1993)
76. C. Song, V. Koch, Phys. Lett. B **404**, 1 (1997)
77. J. Letessier, J. Rafelski, nucl-th/0504028
78. A.S. Kapoyannis, C.N. Ktorides, A.D. Panagiotou, J. Phys. G **28**, L47 (2002)
79. A.S. Kapoyannis, hep-ph/0605324
80. Z. Fodor, S.D. Katz, K.K. Szabó, Phys. Lett. B **568**, 73 (2003)
81. N.G. Antoniou, F.K. Diakonos, A.S. Kapoyannis, Proc. 10th International Workshop on Multiparticle Production, Crete, Greece 8–15 June 2002 (World Scientific), p. 201
82. N.G. Antoniou, A.S. Kapoyannis, Phys. Lett. B **563**, 165 (2003)